

- 3 REED, J.C.: 'Side zone automotive radar', *IEEE Aerosp. Syst. Mag.*, June 1998, pp. 3-7
- 4 LINARDOU, I.: 'The Vivaldi antenna: potential applications at millimeterwaves'. PhD dissertation, University of Nice-Sophia Antipolis, November 2000
- 5 GSCHWENDTNER, E., and WIESBECK, W.: 'Low-cost spiral antenna with dual-mode radiation pattern for integrated radio services'. *IEEE Int. Symp. Antennas and Propagation*, July 2000
- 6 RIBO, M., and PRADELL, L.: 'Circuit model for coplanar-slotline tees', *IEEE Microw. Guid. Wave Lett.*, 2000, 10, (5), pp. 177-179

## Harmonic Love wave devices for biosensing applications

M.I. Newton, F. Martin, K. Melzak, E. Gizeli and G. McHale

Simultaneous operation of a Love wave biosensor at the fundamental frequency and third harmonic, including the optimisation of IDT metallisation thickness, has been investigated. Data is presented showing a sequence of deposition and removal of a model mass layer of palmitoyl-oleoyl-sn-glycerophosphocholine (POPC) vesicles while frequency hopping between 110 and 330 MHz.

**Introduction:** A Love wave is produced in a surface skimming bulk wave (SSBW) device when an insulating overlayer with an acoustic shear velocity less than that in the bulk is deposited over the propagation path [1]. The overlayer has the effect of confining energy to the surface and hence acting as a guiding layer. The use of Love wave devices for biosensing applications was first reported in 1992 [2] and has since attracted much attention [3-7]. The surface mass sensitivity of acoustic wave devices is known to increase with frequency [3]. However, for liquid sensing applications only a thin layer of fluid, called the penetration depth, above the sensor is probed [4]. This penetration depth,  $\delta$ , reduces as the frequency increases according to  $\delta = (2\eta/\rho\omega)^{0.5}$  where  $\omega$  is the angular frequency,  $\eta$  is the viscosity and  $\rho$  the density of the fluid. When biological materials such as a vesicle layer are deposited, they may initially be attached to the mass sensitive surface as a series of spheres, in our case of diameter 50 nm, which then can be opened out to form a monolayer or bilayer. The biological mass layer within the penetration depth thus changes and an acoustic signal response is observed [8]. Here we present data showing a Love wave device operated in a frequency hopping mode utilising both the fundamental and third harmonic during a biosensing experiment.

**Experiment:** In this work we have used a split-finger (double-double) interdigital transducer (IDT) design which, for Rayleigh wave devices, is known to resonate with equal strength at both the fundamental frequency and third harmonic. Devices were fabricated on ST-cut quartz with propagation orthogonal to the crystalline X direction, which is known to support a SSBW, and designed for operation at a fundamental frequency of 110 MHz. Each IDT was of length  $40\lambda$  and aperture  $65\lambda$  where the wavelength  $\lambda = 45\mu\text{m}$ ; finger widths were  $6.75\mu\text{m}$  and spacings were  $4.5\mu\text{m}$ . The path length was 7 mm and the guiding layer consisted of Novolac photoresist dissolved between 5 and 20% (w/v) in 2-ethoxyethylacetate (2-EEA) and spin coated at 4000 rpm for 40s; after deposition the films were cross linked by baking in an oven at 200°C for 2h. Prior to the biosensing experiment these layers were made hydrophilic by treatment with a sol-gel derived silica coating. Hydrochloric acid was used to accelerate and polymerise a silica solution. The gel was then placed on the Novolac surface for 1 min and washed off with deionised water. A flow cell configuration was used for the biosensing experiments. A silicone gasket was used to isolate the surface acoustic wave (SAW) path from the IDTs and liquid was passed through the flow cell at a rate of 0.083 ml/min. The insertion loss of the device was continually monitored using a Hewlett-Packard 4195A network analyser with markers set at the fundamental frequency and third harmonic, effectively hopping between each frequency during the experiment. The experimental sequence consisted of initially a buffer solution,

phosphate buffered saline (PBS), which was then followed by deposition of 0.2 mg/ml of vesicles of palmitoyl-oleoyl-sn-glycerophosphocholine (POPC) in PBS. The vesicle layer was then removed by a detergent, *t*-octyl-phenoxypolyethoxyethanol (Triton) at 0.1% (w/v) in PBS, followed by another sequence of POPC deposition and removal.

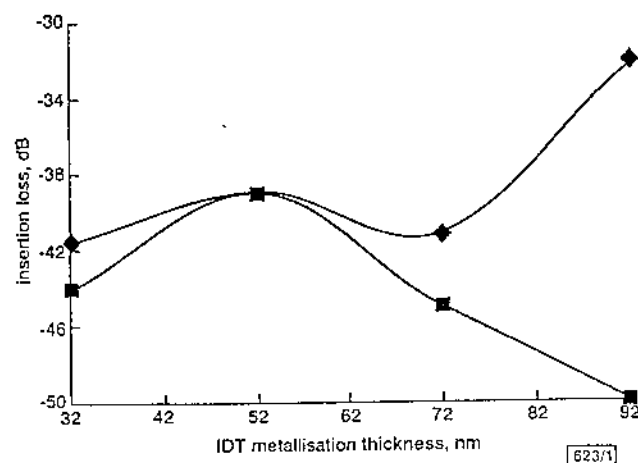


Fig. 1 Insertion loss for fundamental frequency and third harmonic as function of IDT metallisation thickness

◆ fundamental frequency  
■ third harmonic

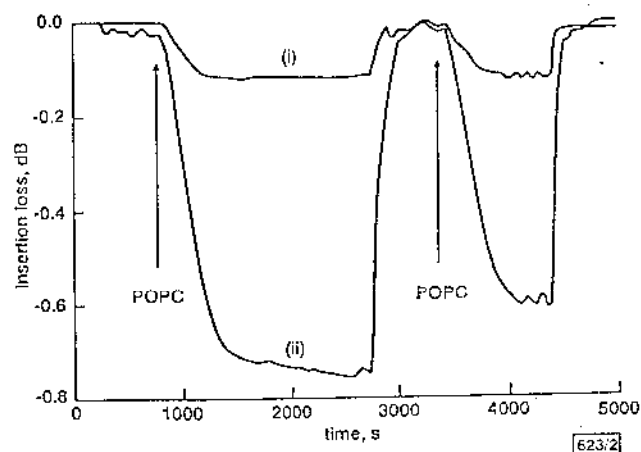


Fig. 2 Change in insertion loss as function of time for two POPC depositions and removal using a fundamental frequency of 110.925 MHz and third harmonic of 332.325 MHz:

(i) fundamental frequency of 110.925 MHz  
(ii) third harmonic of 332.325 MHz

**Results and discussion:** To operate a Love wave device at harmonic frequencies, both the IDT metallisation thickness and guiding layer thickness must be optimised. Fig. 1 shows the effect of IDT metallisation thickness on the insertion loss at both the fundamental and third harmonic. Previous work [9] has shown that the metallisation thickness of the grating is a critical parameter for surface transverse wave (STW) filter operation on this substrate with the third harmonic diminishing with increasing thickness. Our data confirms that is also the case for the IDT thickness for our uncoated SSBW device. All devices used a gold capping layer of 12 nm with a Ti underlayer varied between 20 to 80 nm; from the data in Fig. 1, an IDT metallisation thickness of 52 nm was chosen for all subsequent experiments. The effect of the Love wave guiding layer thickness was also investigated and the optimum value for observing the third harmonic while still retaining a significant fundamental was found to be obtained with 10% Novolac in 2-EEA. Fig. 2 shows the change in insertion loss as a function of time for a typical biosensing experiment. The mass sensitivity is known to increase with operating frequency and this is shown in a factor of five greater change in insertion loss for the harmonic (332.325 MHz) than the fundamental (110.925 MHz). The rise to the initial insertion loss after the detergent treatment suggests that the POPC is fully removed by the Triton. The greater attenuation obtained during the first POPC deposition is consistent with previously published data [8].

**Conclusion:** We have demonstrated the possibility of frequency hopping between the fundamental frequency and third harmonic of a Love wave device during the deposition and removal of a biological mass layer. The optimum interdigital transducer metallisation and guiding layer thickness for simultaneous operation at these frequencies has been investigated.

**Acknowledgment:** The authors gratefully acknowledge the financial support of BBSRC provided by research grant 301/E11140.

© IEE 2001  
*Electronics Letters Online No: 20010243*  
 DOI: 10.1049/el:20010243

M.I. Newton, F. Martin and G. McHale (*Department of Chemistry and Physics, The Nottingham Trent University, Clifton Lane, Nottingham, NG11 8NS, United Kingdom*)

E-mail: michael.newton@ntu.ac.uk

K. Melzak and E. Gizeli (*Institute of Biotechnology, University of Cambridge, Tennis Court Road, Cambridge, CB2 1QT, United Kingdom*)

**References**

- 1 GULYAEV, Y.V.: 'Review of shear surface acoustic waves in solids', *IEEE Trans. Ultrason. Ferroelectr. Freq. Control*, 1998, 45, pp. 935-938
- 2 GIZELI, E., STEVENSON, A.C., GODDARD, N.J., and LOWE, C.R.: 'A novel Love-plate acoustic sensor utilizing polymer overlayers', *IEEE Trans. Ultrason. Ferroelectr. Freq. Control*, 1992, 39, pp. 657-659
- 3 HERMANN, F., HAAN, D., and BUTTGENBACH, S.: 'Separation of density and viscosity influence on liquid-loaded surface acoustic wave devices', *Appl. Phys. Lett.*, 1999, 74, pp. 3410-3412
- 4 JACOBY, B., and VELLEKOOP, M.J.: 'Viscosity sensing using a Love-wave device', *Sens. Actuators A, Phys.*, 1998, 68, pp. 275-281
- 5 WEISS, M., WELSCH, W., SCHICKFUS, M.V., and HUNKLINGER, S.: 'Viscoelastic behavior of antibody films on shear horizontal acoustic surface wave sensors', *Anal. Chem.*, 1998, 70, pp. 2881-2887
- 6 JACOBY, B., and VELLEKOOP, M.J.: 'Analysis and optimization of Love wave liquid sensors', *IEEE Trans. Ultrason. Ferroelectr. Freq. Control*, 1998, 45, pp. 1293-1302
- 7 HARDING, I.G., and DU, J.: 'Design and properties of quartz-based Love wave acoustic sensors incorporating silicon dioxide and PMMA guiding layers', *Smart Mater. Struct.*, 1997, 6, pp. 716-720
- 8 GIZELI, E., LOWE, C.R., LILEY, M., and VOGEL, H.: 'Detection of supported lipid layers with the acoustic Love waveguide device: application to biosensors', *Sens. Actuators B, Chem.*, 1996, 34, pp. 295-300
- 9 BAER, R.L., and FLORY, C.A.: 'Harmonic operation of STW filters', *IEEE Symp. Ultrasonics*, 1988, pp. 53-56

**Temperature retrieval algorithm for brain temperature monitoring using microwave brightness temperatures**

G.M.J. Van Leeuwen, J.W. Hand, J.B. Van de Kamer and S. Mizushima

A solution to the inverse problem of retrieving temperature from a set of microwave brightness temperatures together with *a priori* information regarding weighting functions and heat transfer within the infant head is introduced. The method offers the basis for non-invasive temperature monitoring appropriate for hypothermal neural rescue therapy.

**Introduction:** Cooling of the brain after asphyxia at birth reduces the development of brain damage [1]. Clinical trials investigating the efficacy of brain cooling require that temperatures in the deep brain can be monitored. We are developing a microwave radiometry (MWR) system with five frequency bands for the non-invasive and prolonged monitoring of deep brain temperature [2]. Here we report an improved method for retrieving tissue temperatures from MWR measurements, and examine how uncertainties in measured brightness temperatures and in the data used in the analysis affect the retrieved temperatures.

**Microwave radiometry:** The measured brightness temperature in MWR is defined by the tissue's thermal radiation and is, according to the Rayleigh-Jeans law, proportional to the absolute temperature:

$$T_{B,i} \equiv \frac{P_i}{k\Delta f_i} = \iiint_{afv} W_i(\mathbf{r})T(\mathbf{r})dV \quad (1)$$

where  $P_i$  is the thermal power received by the radiometer's antenna in a bandwidth  $\Delta f_i$  centred around frequency  $f_i$ , and  $k$  is Boltzmann's constant. The rightmost term involves integration over the antenna's field of view (afv) of the product of absolute temperature  $T$  and the radiometric weighting function  $W_i$ . The frequency dependence of  $W_i$  allows extraction of the temperature-depth profile in the tissue from a set of measurements made at different frequencies.

The radiometer antenna is a ceramic loaded open-ended rectangular waveguide. A thin water bolus between the antenna and the baby's head ensures predictable coupling. Each of five receivers, with central frequencies 1.2, 1.65, 2.3, 3.0, and 3.6GHz and 0.4GHz bandwidth, contains a reference noise source that is temperature controlled so as to 'balance' the thermal noise radiation from the antenna. When this condition is met, the brightness temperature of the tissues under observation is equal to that of the reference noise source [3]. For our system, which uses integration times of 4 or 5s, we have calculated the total uncertainty in the measurement of the brightness temperatures to range between 60mK for the 1.2GHz-centred band and 65mK for the 3.6GHz-centred band.

**Modelling:** To calculate brightness temperatures, the weighting functions and temperature distribution must be determined. Electromagnetic and thermal computations were carried out using a 3D anatomically realistic model of an infant head. The radiometric weighting function was found using the reciprocity theorem by calculating the normalised power absorption rate distribution when the antenna was operating as a source rather than as a receiver:

$$W_i(\mathbf{r}) = \frac{(1/2)\sigma_i|\mathbf{E}_i(\mathbf{r})|^2}{\iiint_{afv}(1/2)\sigma_i|\mathbf{E}_i(\mathbf{r})|^2dV} \quad (2)$$

where  $E_i$  is the electric field intensity induced by the antenna and  $\sigma_i$  is the tissue conductivity. The FDTD method with retarded time absorbing boundary conditions [4] was used to calculate the E-field distributions. Excitation of the antenna was modelled by prescribing E-field values for all voxels in the respective probe plane of the waveguide antenna. Temperature distributions within our infant head model were calculated using the heatsink approach [5] and were validated by comparison with those derived using a model that accounted for the effects of discrete vasculature [6]. The base set of thermal boundary conditions represented a cooling cap at 16°C and body core temperature maintained at 34°C.

**Temperature retrieval:** The inverse problem of finding the best estimate for the temperature distribution requires parameterisation of the 3D temperature distribution. In view of the long computation time necessary to calculate a temperature distribution, varying a parameter in the thermal model is not an option for real-time temperature retrieval. Instead, we use pre-calculated distributions  $T_1, T_2, \dots$ :

$$T_{retrieved}(\mathbf{r}) = T_0 + p_1(\Delta T_1(\mathbf{r})) + p_2(\Delta T_2(\mathbf{r})) + \dots \quad (3)$$

where  $T_0$  is the cooling cap temperature,  $\Delta T_i = T_i(\mathbf{r}) - T_0$ , and the  $p_i(T)$  are polynomial functions, the coefficients of which are the parameters to be determined. The parameters can now be taken outside of the volume integral in eqn. 1, which allows the volume integration of the product of weighting function and temperature to be performed before measurements start. For example, two pre-calculated temperature distributions can be used with dimensionless parameters  $a_1$  and  $a_2$  which scale the distributions:

$$T_{retrieved}(\mathbf{r}|a_1, a_2) = T_0 + a_1\Delta T_1(\mathbf{r}) + a_2\Delta T_2(\mathbf{r}) \quad (4)$$

The numerical brightness temperatures can then be written as

$$T_{B,i}(a_1, a_2) = T_0 + a_1 \iiint \Delta T_1 W_i dV + a_2 \iiint \Delta T_2 W_i dV \quad (5)$$